Characterizing the automatic radon flux Transfer Standard system *Autoflux*: laboratory calibration and field experiments

Claudia Grossi[1,2], Daniel Rabago[3], Scott Chambers[4], Carlos Sáinz[3], Roger Curcoll[1], Peter PS. Otáhal[5], Eliška Fialová[5,6], Luis Quindos[3], Arturo Vargas[1]

[1] Institut de Tècniques Energètiques, Universitat Politècnica de Catalunya, 08028 Barcelona, Spain
[2] Physics Department, Universitat Politècnica de Catalunya,08028 Barcelona, Spain
[3] Universidad de Cantabria, 39011 Santander, Spain
[4] ANSTO, Environmental Research, Lucas Heights, NSW 2234, Australia
[5] Nuclear Protection Department, National Institute for Nuclear, Chemical & Biological Protection, Milin 26231, Czech Republic
[6] Department of Geological Sciences, Faculty of Science, Masaryk University, 60200 Brno, Czech Republic

Correspondence to: Claudia Grossi (claudia.grossi@upc.edu)

Abstract

High-quality, long-term measurements of terrestrial trace gas emissions are important for investigations of atmospheric, geophysical and biological processes to help mitigate climate change, protect the environment, and the health of citizens. High-frequency terrestrial fluxes of the radioactive noble gas ^{222}Rn, in particular, are useful for validating radon flux maps, used to evaluate the performance of regional atmospheric models, to improve greenhouse gas emission inventories (by the Radon Tracer Method) and to determine Radon Priority Areas for radiation protection goals.

A new automatic radon flux system (the *Autoflux*) was developed as a Transfer Standard (TS) to assist with establishing a traceability chain for field-based radon flux measurements. The operational characteristics and features of the system were optimized based on a literature review of existing flux measurement systems. To characterize and calibrate the *Autoflux* a bespoke radon Exhalation Bed (EB) facility was also constructed with the intended purpose of providing a constant radon exhalation under a specific set of controlled laboratory conditions. The calibrated *Autoflux* was then used to transfer the derived calibration to a second continuous radon flux system under laboratory conditions, both instruments were then tested in the field and compared with modeled fluxes.

This paper presents: i) a literature review of state-of-the-art radon flux systems and EB facilities; ii) the design, characterization and calibration of a reference radon EB facility; iii) the design, characterization and calibration of the *Autoflux* system; iv) the calibration of a second radon flux system (*INTE_Flux*) using the EB and *Autoflux*, with a total uncertainty of 9% (k=1) for an average radon flux of ~1800 mBq m^{-2} s^{-1} under controlled laboratory conditions; and iv) an example application of the calibrated TS and *INTE_Flux* systems for in situ radon flux measurements which are then compared with simulated radon fluxes. Calibration of the TS under different environmental conditions and at lower reference fluxes will be the subject of a separate future investigation.

1 Introduction

The radioactive, noble gas radon (^{222}Rn) contributes over half of the total public radiation dose from natural sources (WHO, 2009). However, due to its short half-life (3.8 days) and chemical inertness, radon is also widely used as an environmental tracer for atmospheric and geophysical processes (Grossi et al., 2012; Vargas et al., 2015, Chambers et al., 2016; Chambers et al., 2018; Zhang et al., 2021). In particular, climate scientists are using co-located measurements of atmospheric radon and greenhouse gas (GHG) concentrations to apply the so-called Radon Tracer Method (RTM) for estimating local- to regional-scale GHG emissions (Grossi et al., 2018; Levin et al., 2021).

These applications require information, at high temporal resolution and low uncertainty, about: i) the quantity of radon emitted per unit area and time from a surface of interest (the radon flux, *F*, or exhalation rate; usually expressed in mBq m^{-2} s^{-1}); and ii) the atmospheric radon activity concentration (SI units Bq m^{-3}).

Terrestrial radon exhalation is the result of ^{222}Rn escape from soil pore spaces to the atmosphere after its formation by ^{226}Ra decay (Nazaroff, 1992). ^{222}Rn exhalation rates are primarily driven by diffusion processes and depend strongly on the soil ^{226}Ra content and soil properties (porosity, tortuosity, soil humidity, etc.). Consequently, the ^{238}U content and parameters influencing diffusive transport in the soil need to be known to properly estimate the spatial and temporal variability of ^{222}Rn exhalation rates (Schüßler, 1996; Lopez-Coto et al., 2013; Karstens et al., 2015). Furthermore, the emanation factor of radon from the soil grains to the pore spaces is influenced by soil humidity (Nazaroff, 1992; Zhuo et al., 2006; Zhuo et al., 2008).

Although diffusion is the primary transport mechanism of radon in soils, driven by the strong vertical concentration gradient (Karstens et al., 2015), advective transport can also occur, but this has not been thoroughly investigated and is likely to be highly site specific. Advective transport typically results from local pressure gradients, changing wind speed and direction, etc. Consequently, advective processes could influence radon flux measurements (Gutiérrez-Álvarez et al. 2020a). Other factors including soil type, atmospheric pressure, rainfall (related to soil moisture), and soil temperature can affect the radon flux. However, complex dependencies between these factors makes it difficult to quantify changes in radon flux due to any one of these factors in isolation (e.g., a precipitation event is often also associated with a drop in pressure and temperature).

To date, most radon flux studies have been based on random sampling and short temporal measurement data, due to the lack of robust continuous radon flux systems. Unfortunately, these kinds of datasets are not sufficient to clarify relationships between radon flux and environmental factors. This is also a contributing factor to why some studies reach contradictory conclusions about the influence of individual parameters on the radon flux.

Long-term, reliable radon flux measurements are needed in conjunction with corresponding environmental observations in the soil and lower atmosphere (McLaughlin, 2011; Yang et al., 2017). To ensure reliable measurements it is important to characterize and calibrate the operational radon flux systems, which requires: i) a ^{222}Rn Exhalation Bed (EB) facility, to provide reference radon fluxes under controlled laboratory conditions; ii) a Transfer Standard (TS) instrument to be calibrated using the EB and used as a reference monitor for calibrating other new or existing monitors, or to be used directly for in situ measurement campaigns; and iii) planned field-based inter-comparison campaigns of different radon flux systems under in situ environmental conditions.

The need of an EB facility is justified because, despite the fact that the response of the radon monitors itself can be previously studied within a STAR (System for Test Atmospheres with Radon) by comparison with a known reference radon concentration, and that geometries of external volumes making the radon flux systems could be measured separately with their own uncertainties, the total tubes and internal volumes estimation could lead to high uncertainties Thus, comparing the radon flux systems response with reference exhalation bed will allow to characterize the effective height of the systems, needed for the flux calculation, with the minimum uncertainty.

One of the main aims of the EMPIR 19ENV01 project (henceforth traceRadon), which started in June 2020, was to provide the necessary measurement infrastructure and transfer standards to enable traceable radon flux and atmospheric radon activity concentration measurements. These goals are being achieved in collaboration with, among other research groups, the Integrated Carbon Observation System (ICOS, www.icos-cp.eu) network, whose researchers are interested in introducing treaceable radon flux and atmospheric radon concentration measurements to sites within this network for RTM applications.

The specific contributions of this study to the overall traceRadon objectives are to offer a calibrated and characterized continuous TS system, equipped with soil and atmosphere sensors, that can be used to carry out radon flux campaigns at different sites to help improve and evaluate the performance of contemporary radon flux maps and models (Szegvary et al., 2009; Karstens et al., 2015), as well as be used to calibrate other radon flux systems under laboratory or field conditions.

The remainder of this manuscript is arranged in the following way: first, a review is made of state-of-the-art EB facilities, including a description of the one newly designed, built and characterized by Cantabria University for the traceRadon project; next, a review is presented of contemporary, available state-of-the-art radon flux systems, including a description of the new automated system (*AutoFlux)* designed, characterized and calibrated by the Australian Nuclear Science and Technology Organization (ANSTO) and the Universitat Politècnica de Catalanuya (UPC); next, the protocol applied to calibrate another automatic radon flux system (*INTE_Flux*), designed by the Institute of Energy Technologies of the UPC, using the *AutoFlux* and the UC EB facility is described. Finally, both radon flux systems are tested during a field-based intercomparison campaign and the results compared with previous tests of these systems and with radon flux model outputs available at the ICOS Carbon Portal (www.icos-cp.eu/).

2 Materials and Methods

2.1. Overview of theoretical radon flux estimation

A review of relevant literature found that radon flux studies have historically been carried out using a theoretical value as a reference. IAEA (1992) suggested that radon flux systems should be calibrated using a thin layer model, under the assumption of 'pure' diffusion and a soil with well characterized ^{226}Ra activity concentration, depth (thickness), porosity, and radon emanation characteristics (UNSCEAR, 1988; Rogers & Nielson, 1991; Nazaroff, 1992; Porstendörfer, 1994). In contrast, most contemporary radon flux studies have been based on the experimental accumulation chamber method (Hassan et al., 2009), resulting in a standard method reflected in the ISO 11665-7:2012: *Accumulation method for estimating surface exhalation rate*. In these cases, the reference value used for calibration of the radon flux system, and method of flux measurement, is based on the results of an exponential fit of the increasing radon activity concentration inside a chamber of known volume, or in a STAR (ISO, 2009), during several days.

The theoretical approach enables calculation of the radon flux (F) by the diffusion equation (Porstendörfer, 1994):

$$F = \varepsilon \cdot C_{\mathrm{Ra}} \cdot \rho \cdot L \cdot \lambda \cdot \tanh\left(\frac{z}{L}\right) \quad (1)$$

where ε is the radon emanation factor, C_{Ra} is the ^{226}Ra activity of the soil (Bq kg^{-1}), ρ the dry bulk density (kg m^{-3}) of the soil, L the radon diffusion length in the soil (m), z is the soil thickness (m) and λ is the radon decay constant ($2.0993 \cdot 10^{-6}$ s^{-1} following Morawska, 1989).

Within Eq. 1, the emanation factor is defined to be the fraction of radon atoms produced by radium disintegration that escape into the soil pore space. Its value varies between 0, when radon does not escape the ^{226}Ra-containing soil grain, and 1, when all radon escapes. This factor depends on many things, including: grain size and shape, moisture content, porosity, permeability, and the distribution of ^{226}Ra atoms in the mineral grains (Baskaran, 2016).

Considering a soil sample of a determinate mass, where the sample is sufficiently well distributed to ensure that all radon atoms successfully entering the pore spaces of the sample will eventually escape to the air volume and be measured, the emanation factor ε can be defined as:

$$\varepsilon = \frac{A_{\mathrm{Rn}}}{A_{\mathrm{Ra}}} \quad (2)$$

where A_{Ra} is the total radium activity of the sample, and A_{Rn}, the radon activity that escapes from the sample. The radium activity is usually measured by gamma spectrometric analysis of the soil sample (i.e., Quindos et al., 1994). To determine the radon activity that escapes from the sample, an airtight stainless-steel container of known volume is commonly used, and the rate of escape is determined by the increase in radon concentration inside (i.e., Stoulos et al., 2004).

The bulk density, ρ, can be calculated from the sample weight and volume of the dry soil (Hosoda, 2007). When the soil thickness is much smaller than the radon diffusion length (i.e., $z \ll L$), as is the case for the Exhalation Bed used in this study, the approximation $\tanh(z/L) \approx z/L$ can be used. Thus, the final equation will be (Lopez-Coto et al., 2009):

$$F = \varepsilon \cdot C_{\mathrm{Ra}} \cdot \rho \cdot \lambda \cdot z \quad (3)$$

In order to prove the applicability of Eq. 3, the diffusion length L has to be evaluated and compared with z. L can be estimated as:

$$L = \sqrt{D/\lambda} \quad (4)$$

where D is the effective diffusion coefficient of the trace gas in the soil air (hereafter also named effective diffusivity). D is assumed to be constant with depth (Karstens et al., 2015), and can be estimated from water saturation w_s and porosity p using the following expression (Rogers and Nielson, 1991; Prasad et al., 2012):

$$D = D_{air} \cdot p \cdot \exp(-6 w_s p - 6 {w_s}^{14p}) \quad (5)$$

where D_{air} is the radon diffusion coefficient in air ($1.1 \cdot 10^{-5}$ m^{2}s^{-1}).

Karstens et al., (2015) made reference to Jin and Jury (1996) and Millington and Quirk (1960) who proposed, and verified, another experimental estimation of the effective diffusivity:

$$D = D_{air} \cdot \frac{(p-w_V)^2}{p^{2/3}} \quad (5a)$$

where w_V (m^3/m^3) is the Volume Water Content (VWC) of the soil. Equations 5 and 5a were both derived empirically and are quite consistent with each other, mainly for dry soils, as will be shown in the following sections.

The porosity and water saturation w_s (m^3/m^3) (Idoria et al., 2020; IAEA, 2013) are given by:

$$p = 1 - \frac{\rho}{\rho_g} \quad (6)$$

where ρ_g is the grain density, and:

$$w_s = \frac{\rho \cdot w_c}{p \cdot \rho_w} \quad (7)$$

where w_c (kg/kg) is the mass water content of the soil sample and ρ_w is the water density (1000 kg/m^3). Karstens et al., (2015) reported that the temperature dependence of ^{222}Rn diffusivity could also be estimated according to Schery and Wasiolek (1998):

$$D(T) = D_0 \left(\frac{T}{T_0}\right)^{3/2} \quad (8)$$

where T is the mean soil temperature in Kelvin and D_0 the effective diffusivity at the reference temperature T_0= 273 K.

The experimental approach allows the flux of a given soil surface to be calculated from the increase in radon activity concentration $C_{\text{Rn}}(t)$ within a chamber of known volume during a time t, as described by Eq. 9:

$$C_{\text{Rn}}(t) = C_0 e^{-\lambda_{eff} t} + \frac{F \cdot A}{V_{eff} \cdot \lambda_{eff}} \left(1 - e^{-\lambda_{eff} t}\right) \quad (9)$$

where the effective decay constant, λ_{eff}, is the sum of the radon decay constant (λ), possible radon lost due to system leakages (λ_l), and radon concentration reabsorbed by the ground (λ_r), as described by Grossi et al., (2011). C_0 is the initial radon activity concentration within the volume, V_{eff} is the effective volume where the radon is free to accumulate, and A is the area of the exhaling surface.

2.2. State of the art Exhalation Bed facilities

Table S1 in the supplementary material presents a summary of EB facilities found in the literature. The Canadian Mining Institute (CANMET) built a national reference standard flux bed for calibrating flux monitoring instrumentation. This 5 m diameter bed consisted of a 5.5 cm thick layer of uranium bearing material from uranium tailings and provided a radon flux of 285 ± 41 mBq m^{-2} s^{-1} (Stieff et al., 1996). In the University of South China Radon Laboratory a standard facility simulating radon exhalation from soil was built in 2001 (Tan & Xiao, 2011). It consisted of a radon source located at the bottom of a conical volume. The middle cylindrical part was made of a plaster and spumy board that simulates the soil or sand porosity. Finally, in the upper part, there is powdery calcium carbonate to maintain the radon concentration in the conical volume. The reference flux for this system is 1482 ± 50 mBq m^{-2} s^{-1}, which was measured using an activated charcoal box and Lucas cells. It is still operating, and some studies continue to use it (Tan & Xiao, 2013; Tan et al., 2020). Oak Ridge Associated Universities (Tennessee, USA) constructed a multilayer exhalation bed. It consists of a base layer of uranium ore spread over the bottom of a rectangular Hardigg polyethylene case of dimensions 84 cm × 53 cm. The base has a 10 cm covering layer of dirt to create a uniform flux at the top surface. The reference exhalation rate of this system was determined by the accumulation method, using a continuous radon monitor, and by using activated charcoal canisters and electrets. The range of values obtained varied from approximately 80 mBq m^{-2} s^{-1} to 430 mBq m^{-2} s^{-1} (Altic, 2014). Onishchenko et al. (2015), from the Institute of Industrial Ecology UB RAS (Ekaterinburg, Russia), designed a calibration system to test radon flux measurement devices. It was constructed from a 200 L metal drum filled with quartz sand (radium concentration less than 2.5 Bq/kg) with a calibrated ^{226}Ra source in the bottom space of the system. The reference exhalation rate obtained by the accumulation method and charcoal canisters was 700 ± 80 mBq m^{-2} s^{-1}.

Gutiérrez-Álvarez et al. (2020a; 2020b) performed an experimental characterization of a soil exhalation rate using the accumulation method (Eq. 9). Two reference exhalation soils were prepared using phosphogypsum in rectangular polypropylene boxes with 6.0 cm and 13.0 cm soil thicknesses, respectively. Means of the experimental results of the bed exhalation rates were of 13.3 ± 0.4 mBq m^{-2} s^{-1} and 23.4 ± 0.5 mBq m^{-2} s^{-1} with an uncertainty for σ=1 of 2%-3%. These previous values were compared to exhalation rates determined by applying the theoretical approach (Eq. 3) which gave values of 12 mBq m^{-2} s^{-1} and 23 mBq m^{-2} s^{-1}, respectively for the two exhalation beds, with a total uncertainty of about 20%.

2.3. Design of a Reference Radon Exhalation Bed

In the framework of traceRadon, and using information from the previous section, a radon EB was designed and built at the University of Cantabria (UC) following Gutiérrez-Álvarez et al. (2020a; 2020b). The EB structure consisted of five stainless steel plates, welded in the shape of a box, open at the top. In this configuration it is important to minimize air leakages through the plates that may lead to the loss of radon activity. The intended purpose of this EB was to provide a constant, well characterized, radon emanation rate under a specific set of controlled laboratory conditions. Since soil moisture influences on the radon emanation were not of specific interest in this case, a relatively shallow soil matrix was sufficient for the EB aims.

The EB structure was filled with a high ^{226}Ra content soil, extracted from a former Spanish uranium mine in Saelices el Chico (Spain), managed by the Spanish National Uranium Company ENUSA. A total soil mass of around 400 kg was collected. The material was then transported to UC laboratory and distributed over a 30 m^2 plastic surface in a layer of thickness of approximately 1 cm to be dried and homogenized. Soil homogenization was performed according to technical document 1415 (IAEA, 2004) following these steps: i) the material was manually homogenized using a stainless-steel rake; and ii) it was sieved with a 2 mm aperture sieve (the device has a woven wire mesh in accordance with DIN ISO 3310-1). For the sieving process, soil was taken randomly in 5 kg amounts. Finally, the homogenized soil was placed into the EB container.

The EB facility was installed in the basement of the UC Faculty of Medicine, in the Laboratory of Environmental Radioactivity (LaRUC). Sensors were installed to continuously monitor temperature, pressure and soil moisture. Two thermometers (Testo, Model 175T2) measured the soil temperature and air temperature inside the accumulation chambers. Soil moisture was measured with an ODYSSEY (Xtreem) probe, and all environmental parameters were recorded by a data logger every minute. Table S2 of the supplementary material summarizes the main characteristics of the selected sensors.

The EB radon flux was estimated theoretically and experimentally using the approaches presented in Section 2.1. To apply Eq. 3, the various soil parameters were measured and/or calculated as explained in Section 3. The experimental derivation of the EB's radon flux was performed using Eq. 9 as by Gutiérrez-Álvarez et al. (2020a). For this, the whole surface of the EB was covered with a stainless-steel container of known volume (Figure S1 of the supplementary material). Three radon monitors, an RTM 2200 (Sarad GmbH), a Radon Scout (Sarad GmbH) and an AlphaE (Bertin Instruments), were used simultaneously to measure the increase of radon concentration within the effective accumulation volume. Please note that the sum of the volumes occupied by the solid components of the three monitors were lower than 1% of the total available volume of the accumulation chamber. In addition, several small air samples were also taken using the grab sampling technique and analysed with the ionization chamber IK-250 (RADON v.o.s.).

2.4. State of the art in Radon Flux Systems

A literature review carried out in the framework of traceRadon found that radon monitors employed in flux measurement systems mainly fall into two categories: active or passive. Active monitors analyze the air in real time, whereas passive monitors (i.e., charcoal canisters) rely on the progressive accumulation of radon by diffusion. The accumulated radon is then measured using a separate system (e.g., by gamma spectroscopy or ionization chamber) (McLaughlin, 2011). Due to the need of radon flux systems capable of high-frequency measurements (capable of resolving diurnal variability), only active systems will be presented and discussed here.

Generally, radon flux systems are comprised of two main parts: a continuous radon monitor and an accumulation volume to be placed on the soil surface. The radon flux (or exhalation rate), is then calculated by Eq. 9 using the measured increase of radon within the known volume. However, Eq. 9 can only be solved if the exhalation rate F and the total system leakage λ_{eff} remain constant over the designated time period. This condition is hard to satisfy for long-term radon flux measurements under field conditions, making it difficult to apply the ISO suggested exponential fit. Variability of environmental parameters, in the soil and/or atmosphere, may force changes in the quantity of radon exhaled from the surface.Furthermore, gradients of temperature and/or pressure between internal and external air of the accumulation chamber may change the the leakage of the system (λ_{eff}). For short measurement periods, $\lambda_{eff} \cdot t << 1$ and the initial concentration within the accumulation chamber is relatively close to the atmospheric value, which is usually small ($C_0 \approx 0$). Thus, Eq. 9 can be substituted with a Taylor series of the exponential truncated to the first order as:

$$C_{\mathrm{Rn}}(t) = C_0 e^{-\lambda_{eff} t} + \frac{F \cdot A}{V_{eff} \cdot \lambda_{eff}} \left(1 - e^{-\lambda_{eff} t}\right) \approx \frac{F \cdot A}{V_{eff} \cdot \lambda_{eff}} \cdot \lambda_{eff} t = \frac{F}{h_{eff}} \cdot t = b \cdot t \qquad (10)$$

where $h_{eff} = V_{eff}/A$ is referred to as the effective height of the system (Morawska, 1989). Thus, to minimize radon flux and/or λ_{eff} variability during the measurements, it is advisable to perform short radon flux measurements which are also important validate radon flux models.

The main characteristics of radon flux systems in the literature based on continuous radon monitors are summarized here (see Table S3 and Figure S2 of the supplement material for more detail). System 1 was designed and built by ANSTO. While not a commercial system, it is based on a commercial AlphaGUARD (AG) monitor and has a drum-like accumulation chamber with a lid that can be automatically opened and closed. A separate pump is used to circulate air from the accumulation chamber to the AG in a closed loop. No monitoring of the air inside the accumulation chamber is performed by this system. System 2 (the *emanometer*), also designed and built by ANSTO, is the predecessor of the System 1 and is based on the flow-through accumulation method. In this case the accumulation volume is permanently closed and to perform a measurement the edges of the accumulation chamber are buried in soil to make a reasonable seal with the emanating surface (Zahorowski and Whittlestone, 1996). The system has two detection volumes (scintillation cells) separated in the flow path by approximatively 5 minutes to enable separate radon and thoron (^{220}Rn) flux estimation (more details in Zahorowski and Whittlestone, 1996). System 3 is a commercial accumulation chamber designed and built by LI-COR (www.licor.com). To date, this chamber is only sold together with an 8100-401 Chamber Control Kit for the purpose of automatic CO_2 flux measurements. So far it has never been coupled with any commercial radon monitor. Systems 4, 5 and 6 are research products, each using different radon monitors and types of accumulation chambers, some of which can be opened and closed automatically. System 6, in particular, developed at the Helmholtz Zentrum München (Institute of radiation protection), Neuherberg, Germany, allows radon flux measurements to be made at different sites around a circular path, using a mechanical arm (Yang et al., 2017). Unfortunately, system 6 is no longer available due to the discontinuation of the research group. Systems 7 and 8, built by INTE-UPC and UC respectively, are based on radon monitors (DOSEman and AlphaE) operating in diffusion mode. Radon monitors operating in diffusion mode can influence the flux instrument's response time, as well as the subsequent fit calculation for estimating the flux, as will be shown in Section 3. Both systems have accumulation chambers that can only be opened manually, but air is refreshed by an external pump.

The importance of the accumulation chamber characteristics when measuring soil gas fluxes should not be underestimated. An inherent challenge in flux chamber design is minimizing the influence that the chamber may have on the measurements, especially for long-term observations. Based on our literature review, the main characteristics required for radon flux systems (monitors and accumulation chambers) are listed and have been taken into account when developing a radon flux system suitable for use as a Transfer Standard.

For a system capable of making radon flux measurements at high temporal resolution, which minimizes the disturbance of flux estimates by changing environmental parameters inside the accumulation chamber, the main requirements are:

- to use a continuous direct radon monitor that measures activity concentration in flow mode (not diffusion mode) at a high temporal resolution (e.g., 1 min - 10 min), and with a minimum detectable radon activity concentration low enough to measure short term radon increases within the accumulation chamber with a statistical uncertainty lower than 20%, allowing radon flux measurements to be obtained using Eq. 10.
- the accumulation chamber needs to open completely and automatically after each measurement period, to establish the initial condition of C_0 equal to the ambient radon concentration.
- environmental sensors are needed inside and outside the accumulation chamber.
- the accumulation chamber needs to have a smooth internal geometry to avoid inhomogeneous internal concentration distribution.
- the accumulation chamber should be painted gloss white, to minimize the temperature difference between air inside and outside of the chamber when the chamber is in direct sunlight.
- the chamber should have a matching collar to attach to (via an easy to clean and seal flange), which can be firmly seated in the soil (to a depth of 2 cm – 10 cm, depending on soil type / texture) to minimize radon loses (Gutiérrez-Álvarez et al., 2020b).

2.5. Design of a new Radon Flux Transfer Standard (TS) System

Based on the monitor requirements described in section 2.4 an automatic and low maintenance radon flux measurement system was designed and built at ANSTO in September 2020 as an alternative implementation of System 1, described previously. This new system was implemented in collaboration with the UPC, and subsequently fully characterized by UPC in collaboration with UC, in the framework of traceRadon. UPC also implemented the means to remotely control the system for data download during the experiments and improved the scripts for the flux calculations and analysis.

This instrument enables 8 automatic flux measurements to be performed each day, every 3 hours. The *AutoFlux* is comprised of an AG PQ2000 PRO (Saphymo) radon monitor (working in 10 min flow mode), an accumulation chamber (drum) with automatic lid, and several environmental sensors installed within the soil, inside the drum, and outside the drum at 50 cm above ground level. An internal lip near the bottom of the accumulation chamber allows the chamber to be pushed 5 cm into the soil to make a good seal with the surface. The radon flux is estimated by performing linear fit of the radon concentration increase within the closed drum every 10 min over a 1-hour period using Eq. 10. The drum's hinged lid is opened and closed using a 150 lb 4" classic rod linear actuator. The actuator is fitted with an external limit switch kit, powered by a 4 x 12V DC relay card and controlled by a CSI CR1000 datalogger (https://www.campbellsci.es/cr1000). The opening (default 2h) and closing (default 1h) times of the accumulation chamber are adjustable and controlled by the program in the datalogger.

The novelty of this system is that the diurnal and seasonal variability of soil radon fluxes can be observed and studied in parallel with measurements of soil properties and meteorological conditions. The *AutoFlux* system was constructed in such a way that it can perform long-term measurements of radon flux and environmental parameters with almost zero maintenance requirements. Unfortunately, this system does not provide a movable arm to allow a periodic change of the measurement spot. Consequently, the positioning of the lid, even when fully open, can sometimes partially shelter the measurement surface from the rainfall that the surrounding surface is receiving. To best match conditions inside and outside of the chamber when open, the accumulation chamber should be positioned such that the lid opens into the direction of the sun at midday, to maximise the sunlight received by the surface inside.

Figure 1 shows the *AutoFlux* system during a typical radon flux field measurement. Figure S3 of the supplementary material presents a simplified scheme of the actual state of the *AutoFlux* system.

Figure 1. Image of the *AutoFlux* system running in the field. The radon activity concentration, internal air temperature, differential pressure and soil characteristics are measured within the white drum. Ambient temperature, humidity, pressure and rainfall are measured on the side of the transport case (~50 cm a.g.l.), and the main system components are located inside the waterproof transport case.

The air exhaled from the soil, rich in radon and thoron (^{220}Rn), enters the accumulation nominal volume $V_D = 0.02$ m^3 and is pumped at $Q = (1 \pm 0.1)$ L min^{-1} first through a filter (PALL Acro 50) and then through a Permapure PD gas dryer, intended to maintain humidity levels below saturation conditions within the AG monitor. The low humidity air stream then enters a delay volume ($V_{Th} = 6 \cdot 10^{-3}$ m^3) within which the ambient thoron decays. Next, the air passes into the detection volume of the AG ($V_{AG} = 0.62 \cdot 10^{-3}$ m^3) where the radon concentration is measured with a 10-minute temporal resolution. The total volume of the circuit tubes is $V_{Tubes} \approx 0.3 \cdot 10^{-3}$ m^3. The area of the exhaling surface is $A = 0.126$ m^2. Considering the total volume where the radon concentration will be accumulating V_{eff} will be in this case equal to $V_{tot} = V_D + V_{Th} + V_{AG} + V_{Tubes} = 2.6 \cdot 10^{-3}$ m^3 the effective height h_{eff} in the Eq. 10 is equal to 0.204 m.

The drum and soil sensors are installed directly into the soil. All sensor outputs are read by a CR1000 datalogger. A Raspberry Pi 4 (RPi) enables scheduled data downloads from both the CR1000 datalogger and AG via a RS232 serial port and serial to USB FTDI adapter. The RPi, AG, datalogger, PD and all electronic components of the *AutoFlux* system are safety located within a sturdy, waterproof transport case. External sensors are installed on the outer walls of the blue transport case. Table 1 summarizes the sensors installed within the *AutoFlux* system. Data stored on the RPi, which are downloaded from the AG and datalogger hourly, can be transferred to a notebook computer by connecting the RPi with an Ethernet cable, assuming a Bitvise SSh Client is installed.

Figure S4 of the supplementary material shows the accumulation chamber of the *AutoFlux* system in its closed state (left side) and opened state (right side) during a typical radon flux measurement.

Table 1. Sensors installed within the *AutoFlux* system.

Variable (Label within the document)	**Sensor**	**Location**	**Unit (S.I.)**	**Picture**
Volumetric Water Content (VWC) in the soil	CSI CS655 Water Content Reflectometer	Inside Drum	m^3/m^3	
Electrical soil conductivity (EC)	CSI CS655 Water Content Reflectometer	Inside Drum	dS/m	-

Water vapor pressure (VaporPress)	CSI CS655 Water Content Reflectometer	Inside Soil	kPa	-
Soil temperature (T)	CSI CS655 Water Content Reflectometer	Inside Soil	^{0}C	
Drum air temperature (DrumTemp)	SDI-12 sensor Unidata 6508A	Inside Drum	^{0}C	
Atmospheric air Pressure (AtmPress)	Integrated ATMOS-14 sensor	Outside attached to box	mbar	
Ambient air Temperature (AirTemp)	Integrated ATMOS-14 sensor	Outside attached to box	^{0}C	-
Relative Humidity (RH)	Integrated ATMOS-14 sensor	Outside attached to box	%	-
Accumulated rain (Rain)	Hydreon RG-11 Optical Rain Gauge	Outside Drum	mm	
Differential pressure between Drum and external atmosphere (DiffPress)	Novus NP785	Inside/Outside Drum	Pa	

2.6. Calibration of a secondary Radon Flux System using the *AutoFlux* and the UC EB facility

After the characterization of the EB (see Section 3.1), and the calibration of the TS under stable laboratory conditions with a constant reference radon flux (see Section 3.2), they were used together to calibrate a second radon flux system (*INTE_flux*, system 6 of Section 2.3).

The *INTE_flux* system also operates continuously and is capable of making 3 radon flux measurements per day. It consists of a cylindrical metallic chamber connected to two electro valves and a pump. The electro valves and pump are controlled using a Programmable Logic Controller (PLC) and the system is powered via a 30 m water-proof cable. To measure a radon flux with this system, the ^{222}Rn concentration in the chamber exhaled from the soil surface is continuously measured using a DOSEman monitor in diffusion mode, which was previously calibrated at the Radon Reference Chamber (secondary) of the INTE-UPC in agreement with the IEC 61577-4. The DOSEman monitor is powered by an internal battery that lasts 15 days.

A typical calibration experiment setup, as carried out at the UC EB facility, is shown in Figure 2, where the *INTE_Flux* and TS were installed on the EB between the 29th of June 2021 and 1st of July 2021.

Figure 2. Typical calibration experiment carried out at the UC laboratory: the *INTE_Flux* system is installed together with the TS system on the EB facility.

3 Results

3.1. Characterization of the Radon Exhalation Bed (EB) facility

The EB radon flux was determined under laboratory conditions at specific points in time using both theoretical and experimental approaches, as explained in Section 2.1. The necessary parameters to apply Eq. 3 were measured and/or calculated as explained later in this section and are presented in Table 2, along with their respective uncertainties (with k=1). Table 2 also presents all variables and parameters measured or calculated for the experimental characterization of the EB within a week of its installation, together with values obtained from the literature (*D* and λ).

3.1.1 Radium activity concentration (C_{Ra})

The average radium activity concentration of the soil in the EB was obtained by gamma spectrometry analysis of 5 separate samples. The samples were extracted from the center and each of the four corners of the EB at a depth of 10-15 cm. Samples were hermetically sealed in a cylindrical container for one month to allow the ^{226}Ra to reach secular equilibrium with its short-lived progeny (^{214}Pb and ^{214}Bi). After this time, the radium activity was determined using the ^{214}Pb photopeak (351.93 keV) with a high-resolution gamma HPGe coaxial detector (model GL-2015-7500, Canberra, USA) following Celaya et al., (2018). The mean ^{226}Ra activity concentration was 19130 ± 350 Bq kg^{-1}.

3.1.2 Emanation factor (ε)

The initial emanation factor, $\varepsilon_0$of the EB soil was obtained by measuring the ratio between the radon activity (A_{Rn}) within the pores of a small, thin (< 5mm) soil sample and its radium activity (A_{Ra}) (Eq. 2). A_{Rn} in a M = 100 g soil sample was measured by Eq. 9 after hermetically sealing the sample within a volume V = 0.024 m^3 and making an exponential approximation of the radon concentration increase with time. The experiment was repeated n = 3 times.

Each experiment was run over a period of 500 hours and was replicated at standard temperature conditions (T = 298 K) with a dried soil sample. A continuous radon monitor (Radon Scout; Sarad GmbH) was used for these tests after being calibrated in the LaRUC radon chamber (Fuente et al., 2018). A final average emanation factor was obtained as:

$$\varepsilon_0 = \frac{A_{\mathrm{Rn}}}{A_{\mathrm{Ra}}} = \frac{\phi}{\lambda_{eff} \cdot C_{Ra} \cdot M} = \frac{0.032 \cdot 0.024}{2.2 \cdot 10^{-6} \cdot 19130 \cdot 0.1} = 0.18 \tag{11}$$

with ϕ the activity rate of radon (Bq s^{-1}) obtained as the mean of the three exponential fits and λ_{eff} = (2.2 ± 0.3)·10^{-6} s^{-1}, the effective decay constant of the system. The estimated uncertainty of the mean of the initial emanation factor was determined from the the standard deviation of the three experiments and it was equal to 0.03. . It can be observed that $\lambda_{eff} \approx \lambda$, the decay constant of radon, ensuring negligible leakages within the system. A typical measurement experiment is shown in Figure S5 of the supplementary material.

As mentioned in the introduction, the emanation factor could vary over time because – apart from the grain size – it also depends on the moisture content and temperature of the material. Zhuo et al., (2006) and Zhuo et al., (2008) investigated the relationship between the emanation factor variability with soil moisture and soil temperature, and derived the following empirical relationship Eq. 12:

$$\varepsilon = \varepsilon_0 \cdot [1 + a(1 - e^{-bw_s}))] \cdot [1 + c(T - 298)] \qquad (12)$$

where ε is the radon emanation factor estimated for a given temperature T, and ε_0 is the radon emanation factor measured at a temperature of T = 298 K for dried soil (see Eq. 11). w_s is the water saturation fraction and a, b, c are parameters calculated for different types of soil textures and declared by Zhuo et al., (2008).

3.1.3 Bulk density (ρ)

The soil bulk density ρ was calculated by measuring the mass, M, with a calibrated balance, and dividing this by its volume, V_s. The volume was measured from an undisturbed soil sample using a test tube manufactured according to ISO 4788. A value of 1645 ± 2 kg m^{-3} was calculated.

3.1.4 Radon diffusion length (L)

As explained in Section 2, to simplify Eq. 1 to Eq. 3 the soil thickness z of the EB needs to be much smaller than the radon diffusion length L in the material. Equations 4 to 7 had to be applied after measuring and/or calculating the required soil parameters for these equations: water saturation (w_s) and porosity (p) of the soil. In addition, to apply Eq. 6 and 7 the grain density and water content of the soil sample had to be measured. The mass water content w_c (kg/kg) can be measured as the ratio of the mass of water and the mass of dry soil. It is measured by weighing a soil sample, m_{wet}, then drying the sample to remove the water and weighing it again, m_{dry}:

$$w_c = \frac{m_{wet} - m_{dry}}{m_{dry}} \qquad (13)$$

The grain density ρ_g is the ratio of the mass of a dry sample and its volume after eliminating the contribution of the interparticle void volume. It can be calculated from the sample weight m_{dry} and the volume V_{dry} of dry soil from:

$$\rho_g = \frac{m_{dry}}{V_{dry}} \qquad (14)$$

The diffusion coefficient D and the diffusion length L can now be calculated using Eq. 4 and 5 and L is equal to (1.286 ± 0.015) m. The measured EB thickness is equal to (0.165 ± 0.005) m, thus the hypothesis $z << L$ is verified. Using all the previous parameters the radon flux from the EB can be theoretically estimated by Eq. 3 and it is F_{Th_EB} = 1918 ± 278 mBq m^{-2} s^{-1}.

Figure 3 shows the theoretical radon flux of the EB calculated using Eq. 1 assuming that the emanation factor varies according to Eq. 11 of Zhuo et al., (2008). The two versions of radon flux presented in Figure 3 represent changes in the adopted diffusion coefficient D. In one case the flux has been calculated using D from Eq. 5 (blue dots) and the other, D from Eq. 5a (black dots). It is evident that no significant difference in EB flux estimate was observed between these methods in the range of water saturation values for which the EB characterization was performed.

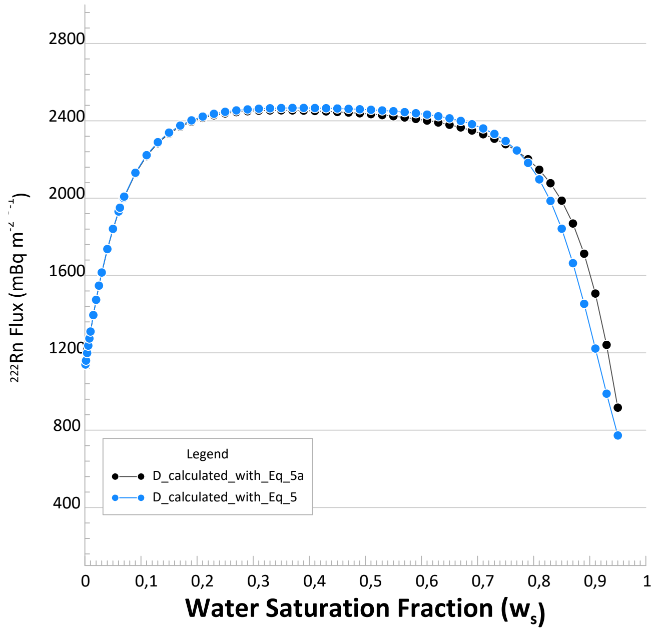

Figure 3. Variability of EB ^{222}Rn flux calculated using Eq. 1 where the emanation factor variability follows Eq. 11 and the diffusion coefficient D was estimated using both Eq. 5 (black dots) and Eq. 5a (blue dots).

As explained in the Methods section, an empirical evaluation of the EB radon flux was also undertaken by enclosing the whole exhaling surface with a cover of known volume. The experiments were performed using different radon monitors inside the closed volume to monitor the radon buildup. Figure S6 of the supplementary material shows the results of a typical accumulation experiment to estimate the EB radon exhalation rate. The experiment was repeated several times to confirm its reliability. The response time of the RTM device was set to 1 minute, while it was 10 minutes for the Radon Scout and AlphaE. Air samples were also collected from the enclosed volume every 15 minutes for independent analysis. Radon concentrations inside the volume reached values of about 130 kBq m^{-3} after only 5 hours. The diffusion mode of operation for the AlphaE and Radon Scout monitors (green and orange dots, respectively in Figure S6) is not capable of correctly representing the temporal variability of radon within the volume, so data from these devices were not used to estimate the EB radon exhalation rate.

The radon exhalation rate was obtained by applying Eq. 10 using parameters summarised in Table 2 (bottom part). Mean values observed by the environmental sensors of the EB facility during the experiments are also reported. The mean of the experiemntal radon flux was $F_{\text{exp\_EB}}$ = 1757 ± 67 mBq m^{-2} s^{-1}.

Table 2. Results of the parameters/variables influencing the calculation/measurements of radon flux from the Exhalation Bed configuration for the theoretical and experimental approaches, respectively. Uncertainties are expressed without any coverage factor (k=1).

Parameter	Symbol	Result
Emanation factor	ε	0.18 ± 0.03
Radium concentration	C_{Ra}	(19130 ± 350) Bq kg^{-1}
Bulk density	ρ	(1645 ± 2) kg m^{-3}
Grain density	ρ_g	(2570 ± 38) kg m^{-3}
Thickness	z	(0.165 ± 0.005) m
Mass Water content	w_c	(0.0132 ± 0.0004) kg/kg
Water saturation	w_s	(0.061 ± 0.008) m^3/m^3
Porosity	p	0.3599 ± 0.0001
Diffusion coefficient	D	(3.47 ± 0.08)·10^{-6} m^2/s
Diffusion length	L	(1.286 ± 0.015) m
Radon decay constant	λ	2.0993(1)·10^{-6} s^{-1}

^{222}Rn Flux	***$F_{Th\_EB} \pm u_{Th\_EB}$***	**1918 ± 278 mBq m^{-2} s^{-1}**
Parameter/Variable	**Symbol**	**Result**
Effective height	h_{eff}	(0.225 ± 0.005) m
Air temperature	T	(20.7 ± 0.3) °C
Mass water content in mass	w_c	(0.013 ± 0.001) kg/kg
Air moisture	RH	(47.0 ± 0.7)%
^{222}Rn Flux	***$F_{Exp\_EB} \pm u_{Exp\_EB}$***	**1757 ± 67 mBq m^{-2} s^{-1}**

3.2 Characterization of the Radon Flux Transfer Standard (TS) System

The *AutoFlux* was characterized and calibrated under controlled laboratory conditions using the EB facility as described previously. Figure S7 of the supplementary material shows the *AutoFlux* setup for a typical laboratory measurement at UC. Two laboratory experiments were performed at standard environmental conditions: i) from the 28th of June 2021 to the 1st of July 2021 (19 radon flux measurements); and ii) from the 7th to the 12th of July 2021 (39 radon flux measurements). Figure 4 shows the radon activity concentrations (upper panels) measured by the *AutoFlux*'s AG during the two continuous experiment periods for each accumulation hour. The bottom panels of Figure 4 show the soil Volume Water Content (*VWC*) time series measured by the CSI CS655 Water Content Reflectometer and the air temperature inside the drum measured by the SDI-12 (Unidata 6508A) sensor during these experiments. A constant increase of around $28 \cdot 10^3$ Bq m^{-3} of radon and of 1 °C of temperature was measured during the 1 h accumulation phase within the system. The Volume Water Content (VWC) measured during the two experiments ranged between 0.025 m^3/m^3 and 0.029 m^3/m^3.

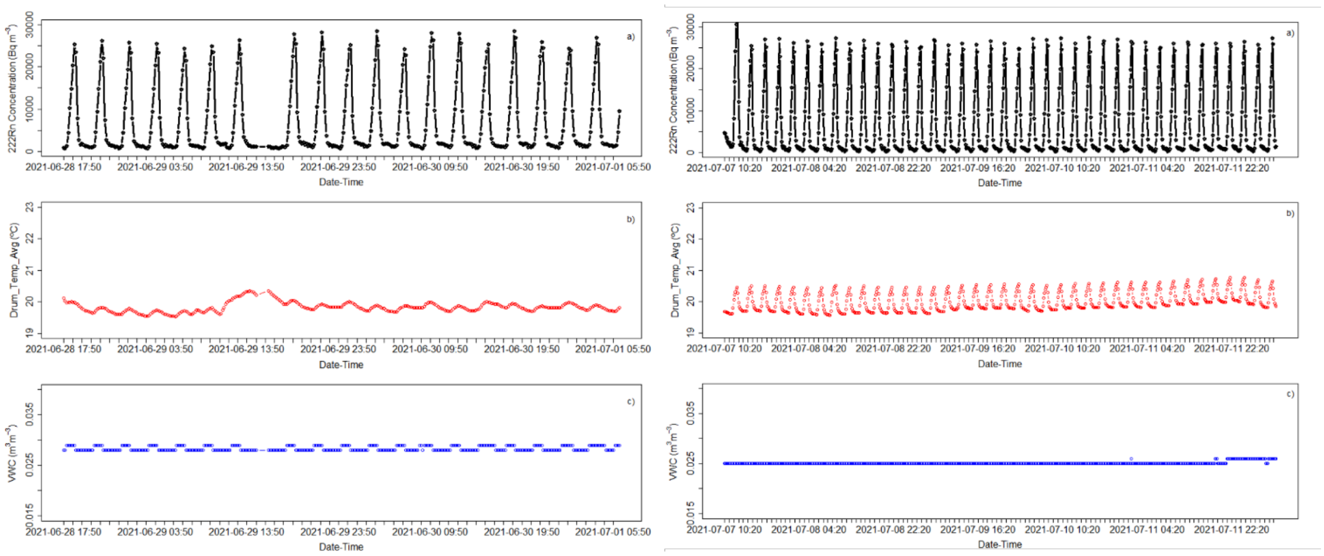

Figure 4. Radon activity concentrations (black dotted lines in panel *a*) measured by the *AutoFlux*'s AG during the two calibration experiments. The bottom panels show the time series of the soil *VWC* (blue dotted lines in panel *c*) and air temperature inside the drum (red dotted lines in panel *b*) during the experiments.

An example of the increase in radon activity concentration measured by the *AutoFlux*'s AG during a typical 1h accumulation period for a single flux measurement is shown in Figure 5. It is evident that the first two values after the chamber closes (0 and 1 in Fig. 5) do not follow the expected theoretical linear increase from Eq. 10. Including these values in the slope calculation could lead to an underestimation of the flux. To better understand the process going on within the drum during a measurement, it is important to note that the 10-minute AG data are representative of the mean radon activity concentration measured over that period, and that the timestamp assigned to each recorded value is at the end of each measurement period. Consequently, the first output value after the chamber is closed (0 in Fig. 5) actually represents the mean radon concentration measured over the 10-minute period leading up to the point of closure. This value has therefore not been considered for the experimental linear fit analysis.

A box model (Eq. 15, 16 and 17 and Figure S8 of the supplementary material) can be used to better understand the behavior of radon activity concentrations in the *AutoFlux* system during the hour of accumulation. Figure S8 shows the three main volumes of the system: V_{AG} is the AlphaGUARD detection volume; V_D is the drum (accumulation chamber) volume and V_u is the total volume of all tubing (V_{tubes}) plus the thoron delay volume (V_{Th}). The change in radon concentration with time in each volume of the system components can be described by the following set of differential Equations:

$$\frac{dC_D(t)}{dt} = \frac{F \cdot A}{V_D} - C_D(t) \cdot \frac{Q}{V_D} + C_{AG}(t) \cdot \frac{Q}{V_{AG}} \quad (15)$$

$$\frac{dC_u(t)}{dt} = C_D(t) \cdot \frac{Q}{V_D} + C_u(t) \cdot \frac{Q}{V_u} \quad (16)$$

$$\frac{dC_{AG}(t)}{dt} = C_u(t) \cdot \frac{Q}{V_u} + C_{AG}(t) \cdot \frac{Q}{V_{AG}} \quad (17)$$

Equations 15, 16 and 17 do not take into account the decay of the radon within these volumes because its will be negligible during the 1h accumulation experiment length. Figure S9 of the supplementary material shows the theoretical increase of radon concentration with time in each of the respective volumes C_D (drum concentration), C_u (concentration in thoron delay and tubes) and C_{AG} (concentration in the AG) during the first hour of system closure, obtained through the analytical solution of Eq. 15, 16 and 17 with the software Mathematica (Wolfram Mathematica). The observed increase in radon within the AG becomes parallel to the radon increase within the accumulation chamber only after 700 sec (≈ 12 minutes). Therefore, the second value measured by the AG after the accumulation volume is closed (point 1 in Figure 5) also can't be considered as part of the experimental linear fit analysis due to the system response time delay.

Looking at Figure 5, the slope of the experimental data (black dotted line) during the accumulation hour, ignoring the first two points (0 and 1) for the reasons mentioned above, gives a radon flux of (1899 ± 60) mBq m^{-2} s^{-1} according to Eq. 10, where the associated uncertainty is calculated from the residual standard error (rse) of the linear fit. These data were measured with a mean volume water content w_V of 0.025 m^3/m^3, equal to a soil water saturation w_s = 0.069 m^3/m^3 that, according to Eq. 1 and 11, gives a theoretical radon flux of (1974 ± 277) mBq m^{-2} s^{-1}. Finally, the experimental data (black dotted line in Figure 5) were fitted with theoretical data (blue dotted line in Figure 5) obtained by solving differential equations 15, 16 and 17 with a radon flux of about (F_{Th_AF} = 1871 ± 187) mBq m^{-2} s^{-1} where the uncertainty of 10% (k=1) is due to the volume estimations and flow variability during the accumulation hour. All of these results are consistent if the associated uncertainties are taken into account and support the understanding of the system response.

Radon concentration time series obtained by exposing the *AutoFlux* system to the UC EB facility (Experiments I and II in Figure 4) were analyzed and Eq. 10 was used to calculate the radon fluxes for each measurement, using only points 2, 3, 4, 5 and 6 of the accumulation phase. This resulted in a mean radon flux of F_{Exp_AF} = 1856 mBq m^{-2} s^{-1} with a standard deviation of $\sigma_{Autoflux}$ = 86.5 mBq m^{-2} s^{-1} over a total of n = 58 radon flux measurements. The error of the mean of the flux measured experimentally by the *Autoflux* monitor will be $u_{Autoflux} = \frac{\sigma_{Autoflux}}{\sqrt{n}} =$ 11.4 mBq m^{-2} s^{-1}. All results are consistent within their respective uncertainties. Finally, Table 3 summarizes the mean radon flux measured by the *AutoFlux* system during experiments I and II at the UC EB facility in October 2021. The means and standard deviations of the variables measured by the *AutoFlux* environmental sensors are also reported.

Table 3. Results of ^{222}Rn fluxes and environmental parameters calculated and/or measured using the *AutoFlux* system during experiments I and II carried out at the UC facility in October 2021 (Grey shaded values have been calculated using Eq. 10 and 15-16-17).

Variable	Mean	St. Dev.
F_{Exp_AF} (mBq m^{-2} s^{-1})	**1856**	**86.5**
F_{Th_AF} (mBq m^{-2} s^{-1})	**1871**	**187**
Flow (L min^{-1})	0.91	0.01
VWC (m^3/m^3)	0.025	0.002
AirTemp (^0C)	19.92	0.095
RH (%)	69.91	1.58
AtmPress (mbar)	1015.3	2.5
DrumTemp (^0C)	20.04	0.11

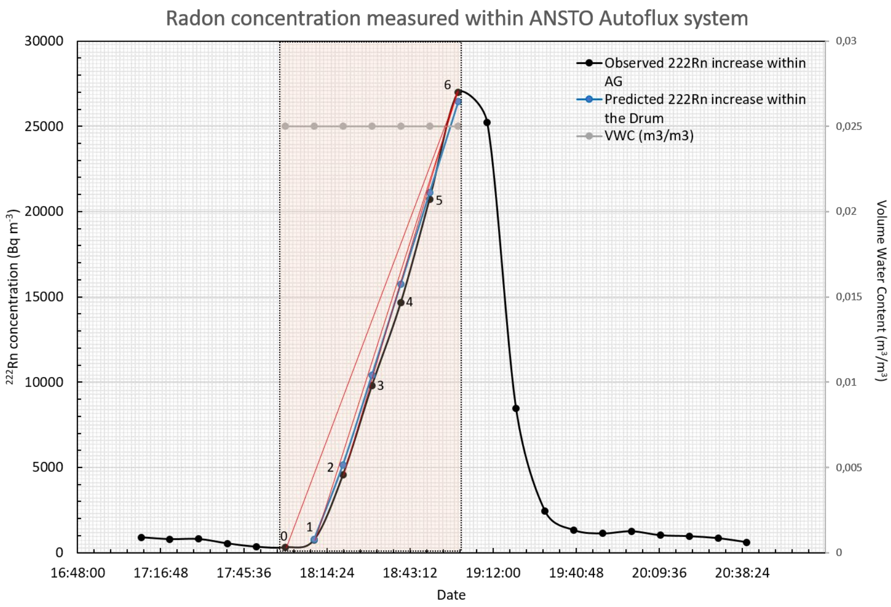

Figure 5. Increase in radon activity concentration within the *Autoflux's* accumulation chamber during a typical radon flux measurement (black dotted line). Blue dotted line represents the theoretical value calculated within the AG volume. The grey dots indicate the *VWC* measured in the soil at the same time. Red lines show different slopes obtained when considering different values.

Considering the agreement between the theoretical and experimental results of the mean radon flux values obtained directly from the EB (F_{Th_EB} and F_{Exp_EB}) or using the *Autoflux* on the EB (F_{Th_AF} and F_{Exp_AF}), the calibration factor of the *AutoFlux* monitor can be now calculated as $F_{Cal\_Autoflux} = F_{Exp\_EB}/F_{Exp\_AF} = 0.95$. The uncertainty of the calibration factor $u_{Cal\_Autoflux} = 0.07$, calculated following the 'Guide to the Expression of Uncertainty in Measurement' (JCGM 100) by Eq. 18:

$$\left(\frac{u_{Cal\_Autoflux}}{F_{Cal\_Autoflux}}\right)^2 = \left(\frac{u_{Autoflux}}{F_{Autoflux}}\right)^2 + \left(\frac{u_{Exp\_EB}}{F_{Exp\_EB}}\right)^2 + \left(\frac{u_{F\_Corr}}{F_{Corr}}\right)^2 \quad (18)$$

It should be noted that F_{Exp_EB} and F_{Exp_AF} were measured within a 1% of variability of the water saturation condition of the emanating soil, which could induce up to a 6% of variability on the measured flux. This possible variability should be considered within the calculation of the uncertainty of the calibration factor of the Transfer Standard monitor, including a correction factor $F_{Corr} = 1$ with un uncertainty $u_{F\_Corr} = 0.06$.

3.3. Calibration of the INTE_Flux system using the TS and the EB facility

The upper panel of Figure 6 shows the radon concentration time series measured at the same time by the DOSEman included within the accumulation chamber of the *INTE_Flux* system and by the AG used for the *AutoFlux* system. The slope b in Eq. 10 can be calculated for each radon accumulation period of the *INTE_Flux* and it has been reported in Table 4, together with the radon fluxes measured by the *INTE_Flux* when a nominal h_{eff} = 0.15 m is applied. The mean value of the radon flux calculated using the *INTE_Flux* system was F_{Client} = 1332 mBq m^{-2} s^{-1} with a standard deviation of σ_{Client} = 140 mBq m^{-2} s^{-1} and the standard error of the mean $u_{Client} = \frac{\sigma_{Client}}{\sqrt{\mathrm{n}}}$ = 63 mBq m^{-2} s^{-1}, where n = 5, the number of radon flux measurements carried out with the *INTE_Flux* system. The mean of the radon flux measured by the TS instrument (*AutoFlux*) during the same period was F_{Ref} = 1868 mBq m^{-2} s^{-1} with a standard deviation of σ_{Ref} = 137 mBq m^{-2} s^{-1} and a standard error of the mean u_{Ref} = 39.5 mBq m^{-2} s^{-1} (n_{Ref} = 12). The calibration factor of the *INTE_Flux* system can be estimated as $F_{Cal} = F_{Ref\_Cal}/F_{Client}$ = 1.33, where $F_{Ref\_Cal} = F_{Ref} \cdot F_{Cal\_Autoflux}$ represents the calibrated radon flux value obtained by the ANSTO *Autoflux* system over the experiment.

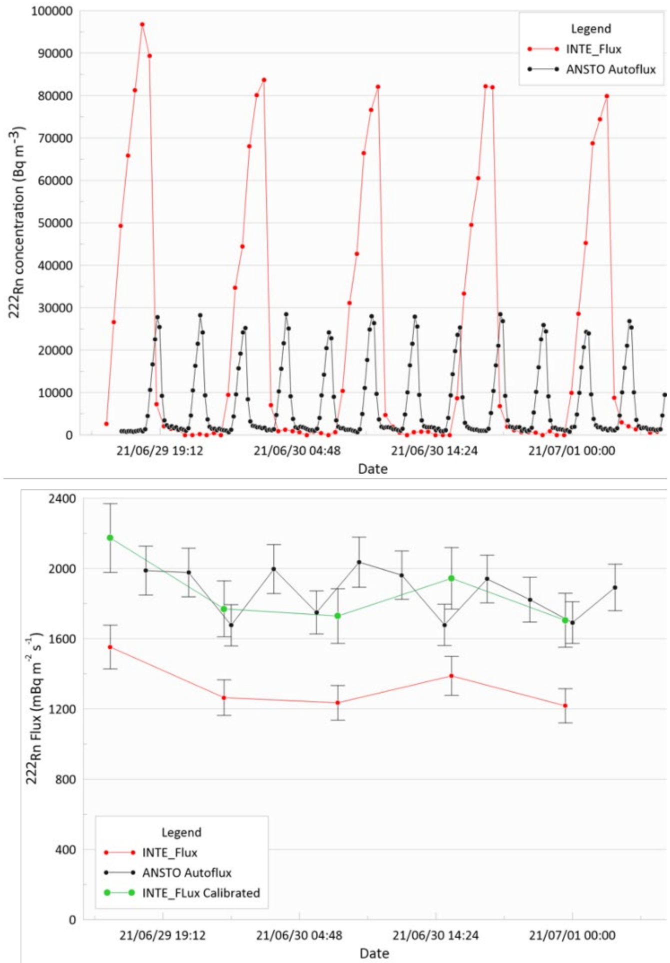

Figure 6. Upper Panel: Time series of radon concentrations measured by the DOSEman (output each 30 min) in the *INTE_Flux* system accumulation chamber and by the AG (output each 10 min) used for the *AutoFlux* on the EB facility of the Cantabria University during the accumulation and ventilation phases of both instruments. Lower panel: Time series of the radon fluxes obtained with the *AutoFlux* system (black dotted line), by the *INTE_Flux* system (*Client*) before the calibration factor being applied (red dotted line) and after its application (green dotted line).

Table 4. Slope and Fluxes obtained by Eq. 10 for the *INTE_Flux* system.

Slope b **(Bq m^{-3} h^{-1})**	F_{Client} **(mBq m^{-2} s^{-1})**
37239	1553
30325	1265
29629	1235
33301	1389
29209	1218
Mean ± Standard Deviation (1332 ± 140) mBq m^{-2} s^{-1}	

To estimate the total uncertainty (u_{cal}) of the calibration factor F_{Cal} in agreement with the 'Guide to the Expression of Uncertainty in Measurement' (JCGM 100) was used Eq. 19:

$$\left(\frac{u_{Cal}}{F_{Cal}}\right)^2 = \left(\frac{u_{Client}}{F_{Client}}\right)^2 + \left(\frac{u_{ref}}{F_{ref}}\right)^2 + \left(\frac{u_{Cal\_Autoflux}}{F_{Cal\_Autoflux}}\right)^2 \qquad (19)$$

Thus, the calibration factor F_{Cal} value will be obtained with a total associated uncertainty equal to $u_{Cal} = 0.12$ which corresponds to 9% of the calibration factor. To ensure a confidence level of 95% the Welch–Satterthwaite equation was used to calculate an approximation to the effective degrees of freedom of the u_{cal} variable and to select the corresponding t-student coverage factor. A total expanded uncertainty $U_{cal} = 0.24$ (k=2) was calculated.

3.4 Short field comparison between TS, *INTE_Flux* and modeled radon fluxes

The calibrated *Autoflux* and *INTE_Flux* systems were used during two intercomparison campaigns presented by Rabago et al., 2022. Figure 7 shows time series of radon concentrations measured within both systems at a low radium content area campaign between the 23rd and the 28th of October, 2021 in Esles de Cayón, Spain (lat.: 43.28, long.: -3.80). Time series of measured VWC and drum temperature from the *Autoflux* are also shown. It can be noted that temperature cycles are mostly related with day/night atmospheric condition where the soil moisture shows a generally decreasing trend over the duration of the campaign. The reader should take into account that the higher radon concentrations measured by the *INTE_Flux* system are inversely proportional to its smaller volume.

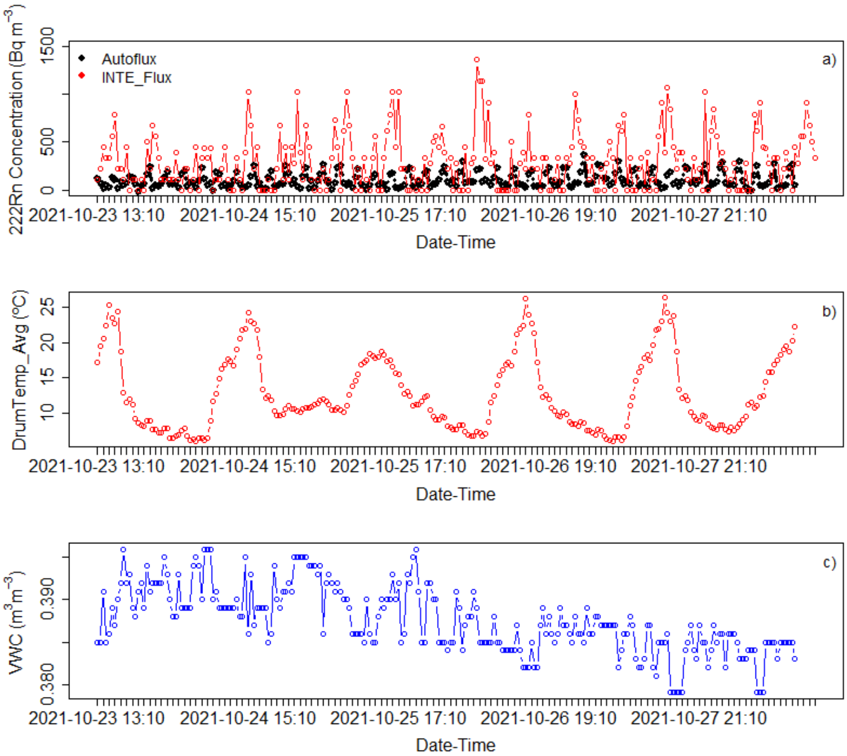

Figure 7. (a) Time series of radon concentrations measured by the *Autoflux's* AG every 10 minutes (black dotted line) and the *INTE_Flux's* DOSEman every 30 minutes (red dotted line), (b) drum temperature (red dotted line), and (c) VWC (black dotted line) measured by *Autoflux* sensors.

Daily mean radon fluxes measured by the *Autoflux* and *INTE_Flux* systems throughout the campaign are shown in Figure 8c together with:

i) Data from the traceRadon daily radon flux maps for Europe 2021 (Figure 8a) based on ERA5-Land and on GLDAS-Noah v2.1 soil moisture reanalysis data (Figure 8b), respectively, available at the ICOS Carbon Portal (Karstens, U. and Levin, I., 2022). Radon fluxes are calculated following Karstens et al., 2015 and including the calculation of the emanation factor proposed by Zhuo et al., 2008 but taking into account only half of the temperature influence (c/2 in Eq. 12). The soil uranium content and the soil proprieties needed to apply Eq. 1 within these maps were extracted by EANR, 2019 and ESDB, Hiederer, 2013, respectively.

ii) Radon fluxes calculated applying the model by Karstens et al., 2015 and the complete emanation factor proposed by Zhuo et al., 2008 with soil temperature and soil moisture values measured by *Autoflux* sensors during the measurement campaign. Uranium content of the soil and soil parameters to apply Eq. 1 were directly measured in the laboratory on soil samples extracted at the measurement site.

It can be observed that radon fluxes measured by the two calibrated systems are in agreement during the field measurements and they increase throughout the campaign in accordance with the decrease in soil water content (Figure 7c). Output of the model based on ERA5_Land and GLDAS_Noah data do not show any increase over the measurement period.. Radon fluxes modeled using GLDAS_Noah reanalysis data or local measured parameters seem to be twice as high as experimental values and ERA5_Land radon flux based data. This might be related to a better estimation of the ERA5_Land soil water content and to an underestimation of the soil water content measured by the one-point sensor of the *Autoflux* and of the GLDAS_Noah data for these days.

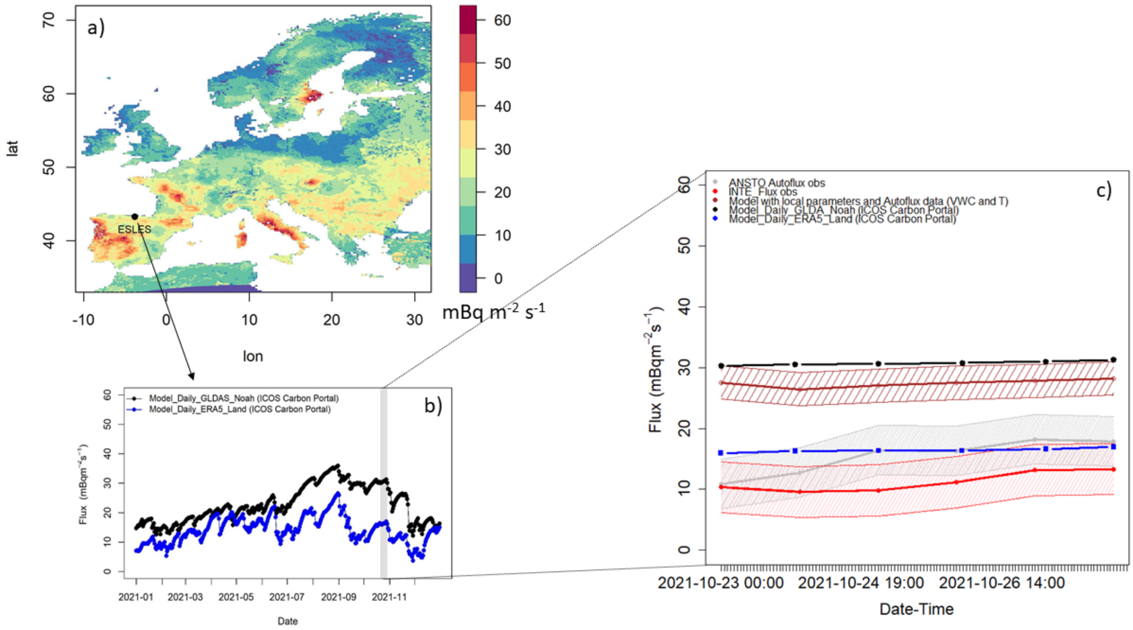

Figure 8. a) Radon flux map for Europe for October 2021 based on GDAS_Noah reanalysis data and Esles location; b) Time series of daily radon fluxes for 2021 modeled using GLDAS_Noah (black dots) and ERA5_Land (Blue dots) reanalysis data at Esles coordinates; c) Daily fluxes and standard deviations of: *Autoflux* observations (black dotted line), *INTE_Flux* observations (red dotted line), model based on measurements (brown dotted line), model based on ERA5_Land reanalysis (orange dotted line) and GLDAS_Noah reanalysis (blue dotted line).

Conclusions

Reliable long-term radon flux observations are important to validate radon flux maps used for radiation protection and climate goals.

In the present study a new automatic radon flux system, which allows 3-hourly measurement of radon fluxes together with environmental parameters in the soil and ambient air, has been characterized and calibrated for being used as Transfer Standard to enable traceable radon flux measurements. This was done using a bespoke exhalation bed built and characterized for this purpose. The new radon flux system (*Autoflux*) was then used to calibrate a second radon flux monitor (*INTE_Flux*). Both calibrated monitors were tested during a short in situ measurement campaign and results were compared with ones obtained from available radon flux maps using soil proprieties from European datasets (traceRadon daily radon flux maps for Europe 2021 based on ERA5-Land and on GLDAS-Noah v2.1 soil moisture reanalysis data, respectively, available at the ICOS Carbon Portal) or local measurements.

The exhalation bed, designed and built as primary standard, was characterized both theoretically and experimentally to check its reliability and to better understand how the variability of some soil conditions, such as the water content, could influence the measured radon exhalation. The experimental approach allows a significant reduction of the uncertainty of the radon exhalation rate.

Based on the results so far, the automatic *AutoFlux* system appears to be a reasonable option for a Transfer Standard, however further studies of this kind should be carried out at lower reference radon exhalation rates (in the order of tens mBq m^{-2} s^{-1}) and under extreme environmental conditions of soil moisture and temperature to better understand sub daily timescale variability of measured fluxes and to quantify the increase of the total flux value uncertainty for these cases. In addition, the *AutoFlux* system, for low radon flux soils, may be used with a continuous radon monitor with a faster response and an higher sensitivity in to allow to observe the linear increase of the radon concentration within the accumulation chamber with the smallest possible standard deviation.

Daily radon flux observations during the short field intercomparison campaign carried out in northern Spain from the two calibrated systems are coherent, within their daily standard deviations, and in agreement with the daily radon fluxes modeled using ER5_Land reanalysis. Daily radon fluxes modeled using local measured parameters and variable or GDAS_Noah reanalysis data show higher values. This last result shows the importance to validate the input parameters (porosity, bulk density, etc.) and variable (i.e. volume water content and temperature in the soil) used within the model and to perform long-term measurements at different soils and under different meteorological conditions.

Author Contributions

C. Grossi, D. Rabago, S. Chambers, R. Curcoll and A. Vargas led the data analysis and the writing of the manuscript. D. Rabago, C. Sáinz and L. Quindos carried out the literature study and the design, building and characterization of the Exhalation Bed facility. P.PS. Otáhale and E. Fialová led the literature study of the radon flux systems. C. Grossi, A. Vargas and D. Rabago carried out the experimental and theoretical characterization of the *Autoflux* system. All authors participated in the discussion of the results and the writing of the manuscript.

Acknowledgments

Authors declare do not have any conflict of interest.

This study has been possible thanks to the project 19ENV01 traceRadon. The project 19ENV01 traceRadon has received funding from the EMPIR programme co-financed by the Participating States and from the European Union's Horizon 2020 research and innovation programme. 19ENV01 traceRadon denotes the EMPIR project reference.

Authors want to thank the work of Sylvester Werczynski, previously employed at ANSTO, who worked on the design and control software of the *Autoflux* system and of Ute Kartsens who made available the radon fluxes model data.

Code and data availability

The data and the codes from this study are available from the corresponding author and at the following link: https://github.com/ClauGro/GRL_Data. Scripts of the software R v. 3.6.2 (with Rstudio) and Phyton v. 3.8 (with Spyder) were used and are also shared in the github repository.

References

Altic, N. A. Pilot study report for radon exhalation measurements. Oak Ridge Associated Universities, Tennessee, dcn: 2052-TR-41-0(RFTA 11-016), 2014.

Baskaran, M. Radon: A tracer for geological, geophysical and geochemical studies. Springer. Detroit (USA). doi: 10.1007/978-3-319-21329-3, 2016.

Celaya González, S., Rábago Gómez, D., Fuente Merino, I., Quindós López, L., Bon Carreras, N., Valero Castell, M. T., Gutierrez Villanueva, J. L. & Sainz Fernández, C. A simple national intercomparison of radon in water. Radiation Protection Dosimetry, 181(4), 343-349, 2018.

Chambers, S.D. Williams, A.G. Conen, F. Griffiths, A.D. Reimann, S. Steinbacher, M. Krummel, P.B. Steele, L.P. van der Schoot, M.V. Galbally, I.E. Molloy, S.B. Barnes, J.E. Towards a universal "baseline" characterisation of air masses for high- and low-altitude observing stations using Radon-222, Aerosol and Air Quality Research 16, 885–899, doi: 10.4209/aaqr.2015.06.0391, 2015.

Chambers SD, Preunkert S, Weller R, Hong S-B, Humphries RS, Tositti L, Angot H, Legrand M, Williams AG, Griffiths AD, Crawford J, Simmons J, Choi TJ, Krummel PB, Molloy S, Loh Z, Galbally I, Wilson S, Magand O, Sprovieri F, Pirrone N and Dommergue A. Characterizing Atmospheric Transport Pathways to Antarctica and the Remote Southern Ocean Using Radon-222, Front. Earth Sci., 6:190, doi: 10.3389/feart.2018.00190, 2018.

Ferry C., Beneito A., Richon P. and Robe M.-C. An Automatic Device for Measuring the Effect of Meteorological Factors on Radon-222 Flux from Soils on the Long-term, Radiation Protection Dosimetry, Volume 93, Issue 3, 1 February 2001, Pages 271–274, doi: 10.1093/oxfordjournals.rpd.a006439, 2001.

Grossi C., Vargas A., Camacho A., Lopez C. I., Bolívar J., Xia Y. and Conen F. Inter-Comparison of Different Direct and Indirect Methods to Determine Radon Flux from Soil. Radiation Measurements. 46. 112-118, doi: 10.1016/J.Radmeas.2010.07.021, 2011.

Grossi, C., Vogel, F. R., Curcoll, R., Àgueda, A., Vargas, A., Rodó, X., and Morguí, J.-A. Study of the daily and seasonal atmospheric CH_4 mixing ratio variability in a rural Spanish region using ^{222}Rn tracer, Atmos. Chem. Phys., 18, 5847–5860, doi: 10.5194/acp-18-5847-2018, 2018.

Gutiérrez-Álvarez, I., Martín, J. E., Adame, J. A., Grossi, C., Vargas, A., & Bolívar, J. P. Applicability of the closed-circuit accumulation chamber technique to measure radon surface exhalation rate under laboratory conditions. Radiation Measurements, 133, 106284, doi: 10.1016/j.radmeas.2020.106284, 2020a.

Gutiérrez-Álvarez, I., Guerrero, J. L., Martín, J. E., Adame, J. A., & Bolívar, J. P. Influence of the accumulation chamber insertion depth to measure surface radon exhalation rates. Journal of hazardous materials, 393, 122344, doi: 10.1016/j.jhazmat.2020.122344, 2020b.

Hassan, N. M., Hosoda, M., Ishikawa, T., Sorimachi, A., Sahoo, S. K., Tokonami, S., and Fukushi, M. Radon migration process and its influence factors; review. Japanese Journal of Health Physics, 44(2), 218-231, doi: 10.5453/jhps.44.218, 2009.

Hosoda, M., Shimo, M., Sugino, M., Furukawa, M., & Fukushi, M. Effect of soil moisture content on radon and thoron exhalation. Journal of nuclear science and technology, 44(4), 664-672, doi: 10.1080/18811248.2007.9711855, 2007.

IAEA. Soil Sampling for Environmental Contaminants, IAEA-TECDOC-1415, IAEA, Vienna, 2004.

IAEA. Measurement and Calculation of Radon Releases from NORM Residues, IAEA-TECDOC-77, IAEA, Vienna, 2013.

Indoria, A. K., Sharma, K. L., & Reddy, K. S. Hydraulic properties of soil under warming climate. Climate Change and Soil Interactions, 473-508, doi: 10.1016/B978-0-12-818032-7.00018-7, 2020.

ISO 61577-7:2009. Equipment for the production of reference atmospheres containing radon isotopes and their decay products (STAR). ISO: Geneva, Switzerland, 2009.

ISO/IEC 13528:2015. Statistical methods for use in proficiency testing by interlaboratory comparison, 2015.

Jin, Y. and Jury, W. A. Characterizing the Dependence of Gas Diffusion Coefficient on Soil Properties, Soil Sci. Soc. Am. J., 60, 66–71, doi: 10.2136/sssaj1996.03615995006000010012x, 1996

Karstens, U., Schwingshackl, C., Schmithüsen, D., and Levin, I. A process-based ^{222}radon flux map for Europe and its comparison to long-term observations, Atmos. Chem. Phys., 15, 12845–12865, doi: 10.5194/acp-15-12845-2015, 2015.

Karstens, U. and Levin, I. traceRadon daily radon flux map for Europe 2021 (based on ERA5-Land soil moisture), https://hdl.handle.net/11676/NvC7D-BVXlnHtFBdUSKpNVHT, Access Date: 22nd August, 2022.

Karstens, U. and Levin, I., traceRadon daily radon flux map for Europe 2021 (based on GLDAS-Noah v2.1 soil moisture), https://hdl.handle.net/11676/JoDR653JxQuqLvEwzqI2kdMw, Access Date: 22nd August, 2022.

Levin, I., Karstens, U., Hammer, S., DellaColetta, J., Maier, F., and Gachkivskyi, M. Limitations of the radon tracer method (RTM) to estimate regional greenhouse gas (GHG) emissions – a case study for methane in Heidelberg, Atmos. Chem. Phys., 21, 17907–17926, doi:10.5194/acp-21-17907-2021, 2021.

López-Coto I., Mas J. L., Bolivar J. P., García-Tenorio A. A short-time method to measure the radon potential of porous materials. Applied Radiation and Isotopes 67, 133–138, doi: 10.1016/j.apradiso.2008.07.015, 2009.

López-Coto, J., Mas, J. L., and Bolivar, J. P. A 40- year retrospective European radon flux inventory including climatological variability, Atmos. Environ., 73, 22–33, doi: 10.1016/j.atmosenv.2013.02.043, 2013.

Mclaughlin T. Technical Bases And Guidance For Radon Flux Monitoring At Uranium Mill Tailing Sites. DOE CONTRACT NO. DE-AC05-06OR23100, (RFTA 11-010) DCN 2042-TR-01-0, 2011.

Millington, R. J. and Quirk, J. P. Transport in Porous media, Proceedings of the 7th International Congress of soil Science, Madison, Wisconsin, USA, 97–106, 1960.

Morawska, L. Two ways of ^{222}Rn determining the emanation coefficient. Health Phys. 57, 481-483, ISSN: 00179078, 1989

Nazaroff, W. W. Radon transport from soil to air. Reviews of geophysics, 30(2), 137-160, doi: doi.org/10.1029/92RG00055, 1992

Onishchenko, A., Zhukovsky, M., & Bastrikov, V. Calibration system for measuring the radon flux density. Radiation protection dosimetry, 164(4), 582-586, doi: 10.1093/rpd/ncv315, 2015.

Porstendörfer, J. Properties and behaviour of radon and thoron and their decay products in the air. Journal of Aerosol Science, 25(2), 219-263, doi: 10.1016/0021-8502(94)90077-9, 1994.

Prasad, G., Ishikawa, T., Hosoda, M., Sorimachi, A., Janik, M., Sahoo, S. K., Uchida, S. Estimation of radon diffusion coefficients in soil using an updated experimental system. Review of Scientific Instruments, 83(9), 093503, doi: 10.1063/1.4752221, 2012.

Quindos, L. S., Fernandez, P. L., Soto, J. A method for the measurement of the emanation factor for ^{222}Rn in small samples of porous materials. Radiation Protection Dosimetry, 56(1-4), 171-173, ISSN 0144-8420, 1994.

Rábago, D. Quindós, L. Vargas, Sainz, C. Radulescu, I. Ioan, I. Cardellini, F. Capogni, M. Celaya, S. Fuente, M. Grossi, C. Intercomparison of Radon Flux Monitors at Low and at High Radium Content Areas under Field Conditions. International Journal of Environmental Research and Public Health, 19(7), 4213. doi: 10.3390/ijerph19074213, 2022.

Rogers, V. C., & Nielson, K. K. Multiphase radon generation and transport in porous materials. Health Physics, 60(6), 807-815, doi: 10.1097/00004032-199106000-00006, 1991.

Röttger, A. Röttger, S. Grossi, S. Vargas A. New metrology for radon at the environmental level, Measurement Science and Technology, 32(12), 124008, doi: 10.1088/1361-6501/ac298d, 2021.

Röttger, S. Röttger, A. Grossi, C. Vargas, A. Karstens, U. Cinelli, G. Chung, E. Kikaj, D. Rennick, C. Mertes, F. Radulescu I. Radon metrology for use in climate change observation and radiation protection at the environmental level. Advances in Geosciences, 57, pp. 37–47, doi: 10.5194/adgeo-57-37-2022, 2022.

Schery, S. D. and Wasiolek, M. A. Radon and Thoron in the Human Environment, chap. Modeling Radon Flux from the Earth's Surface, World Scientific Publishing, Singapore, 207–217, 1998.

Schüßler, W. Effektive Parameter zur Bestimmung des Gasaustauschs zwischen Boden und Atmosphäre, PhD thesis, Heidelberg University, Germany, 1996.

Stefani, N. Likos, W. J. Asce, M. Benson, C. Evaluation of Two Methods for Measuring Radon Flux from Earthen Radon Barriers. Geo-Chicago 2016 GSP 273, 145-155, WoS Id:000389439100016, 2016.

Stieff, L., Kotrappa, P., Bigu, J. Passive E-perm radon flux monitors for measuring undisturbed radon flux from the ground. In Proc. International Radon Symposium, American Assoc. of Radon Scientists and Technologists, Haines City, FL, 1996.

Stoulos, S., Manolopoulou, M., Papastefanou, C. Measurement of radon emanation factor from granular samples: effects of additives in cement. Applied Radiation and Isotopes, 60(1), 49-54, doi: 10.1016/j.apradiso.2003.10.004, 2004.

Szegvary, T. Conen, F. Ciais, P. European 222Rn inventory for applied atmospheric studies, Atmos. Environ., 43, 1536–1539, doi: 10.1016/j.atmosenv.2008.11.025, 2009.

Tan, Y. and Xiao, D. Revision for measuring the radon exhalation rate from the medium surface. IEEE Transactions on Nuclear Science, 58(1), 209-213, doi: 10.1109/TNS.2010.2090897, 2011.

Tan, Y., and Xiao, D. A novel method to measure the radon exhalation rate in only one measurement cycle. Analytical Methods, 5(3), 805-808, doi: 10.1039/C2AY26134K, 2013.

Tan, Y., Yuan, H., Xie, Y., Liu, C., Liu, X., Fan, Z., Kearfott, K. No flow meter method for measuring radon exhalation from the medium surface with a ventilation chamber. Applied Radiation and Isotopes, 166, 109328, doi: 10.1016/j.apradiso.2020.109328, 2020.

UNSCEAR. United Nations Scientific Committee on the Effects of Atomic Radiation. Sources, effects and risks of ionizing radiation. New York. ISBN 92-1- 142143-8, 1988.

Yang J., Buchsteiner M., Salvamoser J., Irlinger J., Guo Q. And Tschiersch J. Radon Exhalation From Soil And Its Dependence From Environmental Parameters, Radiation Protection Dosimetry 177,1-2, 21–25, doi:10.1093/Rpd/Ncx165, 2017.

Zahorowski, W. and Whittlestone, S. A fast portable emanometer for field measurements of radon and thoron flux. Radiation Protection Dosimetry, 67, 2, 109-120, doi: 10.1093/oxfordjournals.rpd.a031802, 1996.

Zhang, B. Liu, H. Crawford, J.H. Chen ,G. Fairlie, T.D. Chambers, S.D. Kang, C.-H. Williams, A.G. Zhang, K. Considine, D.B. Sulprizio, M.P. Yantosca, R.M. Simulation of radon-222 with the GEOS-Chem global model: Emissions, seasonality, and convective transport, Atmospheric Chemistry and Physics 21, 1861-1887, doi:10.5194/acp-21-1861-2021, 2021.

Zhuo, W., Iida, T., and Furukawa, M. Modeling radon flux density from the Earth's surface, J. Nucl. Sci. Technol., ISSN 0022-3131, 43(4), 479-482, 2006.

Zhuo, W., Guo, O., Chen, B., and Cheng, G. Estimating the amount and distribution of radon flux density from the soil surface in China, J. Environ. Radioactiv., 99, 1143–1148, doi: 10.1016/j.jenvrad.2008.01.011, 2008.